ELSEVIER

Journal of Fluids and Structures 22 (2006) 807–818

JOURNAL OF FLUIDS AND STRUCTURES

www.elsevier.com/locate/jfs

Two-degree-of-freedom vortex-induced vibrations using a force assisted apparatus

J.M. Dahl, F.S. Hover, M.S. Triantafyllou*

Department of Mechanical Engineering, Center for Ocean Engineering, Massachusetts Institute of Technology, 77 Massachusetts Avenue, Cambridge, MA 02139, USA

Received 29 September 2005; accepted 11 April 2006
Available online 4 August 2006

Abstract

We report results from two-degree-of-freedom vortex-induced vibration tests on a flexibly mounted, rigid, smooth cylinder in cross-flow. The tests are performed for six in-line natural frequency to transverse natural frequency ratios. The Reynolds number based on diameter ranged from 11 000 to 60 000. To reduce structural damping in both directions, an apparatus utilizing two linear motors was used. Increasing the in-line to transverse frequency ratio caused a shift in the peak amplitude response to increasingly higher reduced velocities; and at a frequency ratio of 1.9, two distinct response peaks appear, in agreement with earlier experiments by Sarpkaya in 1995. Other comparisons are made with the low mass-damping, two-degree-of-freedom experiments by Jauvtis and Williamson in 2004. The frequency ratio affects the phase lag between transverse and in-line oscillations and hence the shape of the cylinder orbital.

Keywords: Vortex-induced-vibrations; 2 DOF; Frequency ratio

1. Introduction

Vortex shedding along a long, flexible, cylindrical structure placed in a sheared cross-flow, is a three-dimensional (3-D) process and the resulting vibration consists of a combination of in-line and transverse oscillations. An experimental simplification of the problem is usually employed by modeling a small portion of the long cylindrical structure, using an elastically mounted, long aspect ratio, rigid cylinder placed in uniform cross-flow. Often, only a transverse response is allowed in the experiments to further simplify the problem.

Flexibly mounted, circular cylinders undergo vortex-induced vibrations when the vortex shedding frequency is sufficiently close to excite the natural frequency of the cylinder structure. The large oscillatory lift force can result in significant transverse (perpendicular to the incoming flow) motions of the cylinder, about one diameter in amplitude, oscillating at the frequency of vortex shedding (Sarpkaya, 1979, 2004). Drag on the cylinder is composed of a steady component and an oscillating component. The oscillating drag component also excites the cylinder in the in-line (parallel to the incoming flow) direction; however, a frequency-doubling occurs in the drag direction, relative to the

*Corresponding author. Tel.: +1 617 253 4335.
E-mail address: mistetri@mit.edu (M.S. Triantafyllou).

0889-9746/$ - see front matter © 2006 Elsevier Ltd. All rights reserved.
doi:10.1016/j.jfluidstructs.2006.04.019

oscillatory lift force. Significant amplitudes of motion can be seen in the in-line direction, although smaller than in the transverse direction.

Since flexible structures often undergo vortex-induced vibrations in two degrees of freedom, it is significant to employ a model rigid cylinder that is elastically mounted in two degrees of freedom. Moe and Wu (1990) considered the free vibrations of a cylinder in two degrees of freedom and found that the vibrations were sensitive to the history of the cylinder motions. Amplitudes of motion would vary significantly, largely affected by previous motions. Moe and Wu (1990) conducted the experiments setting the in-line and transverse natural frequencies to be equal.

A flexible structure, such as a cable, or a long beam-cable, can have multiple natural frequencies in both the in-line and transverse directions. Since the in-line excitation of a cylinder in steady flow has twice the frequency of the transverse excitation, a flexible structure with multiple natural frequency modes may have different mode excitation in the in-line and transverse directions. Even if the nominal ratio between the two frequencies is not exactly equal to two, the large variability of the added mass in the transverse direction can cause the actual frequency ratio to be sufficiently close to two, resulting in significant in-line, as well as transverse resonant response.

Sarpkaya (1995) reported the effect of in-line cylinder motion on transverse motion response in two-degree-of-freedom free vibration tests for a variety of in-line to transverse frequency ratios. The results for a 1:1 frequency ratio and 2:1 frequency ratio were compared with results of a transverse-motion-only response. Sarpkaya (1995) found that allowing in-line motion for the 1:1 frequency ratio case resulted in larger amplitude cylinder motion, relative to transverse-response only, because energy was transferred from in-line motions to transverse motions. The in-line motions also caused a delay in the peak transverse response of the cylinder, with the peak response occurring at a higher reduced velocity when compared with the transverse-motion-only case. For the 2:1 frequency ratio case he observed two distinct peaks in the transverse motion amplitude.

Jeon and Gharib (2001) studied the forced vibrations of a two-degree-of-freedom cylinder in cross-flow. Using observations from previous experiments, Jeon and Gharib (2001) studied the forced vibrations of a circular cylinder with -45° and 0° phase difference between the transverse and in-line motions. The -45° phase difference corresponds to a figure-eight shape with bent lobes facing downstream, while 0° phase results in a symmetric figure-eight shape. Jeon and Gharib (2001) found that in-line motions have a significant effect on the phase of vortex shedding in the wake of the cylinder. The presence of in-line motions caused a significant change in the flow pattern behind the cylinder, causing a delay of the transition from a '2S' pattern (two vortices forming per cycle) to a '2P' pattern (four vortices per cycle), using the nomenclature of Williamson and Roshko (1988). The delay of the onset of the '2P' pattern is significant for the energy balance of the two-dimensional response.

Mode response branches of the wake of a circular cylinder are discussed in Brika and Laneville (1993) and Govardhan and Williamson (2000). Since cylindrical ocean structures have low mass ratios and typically low structural damping, it is desirable to study the characteristics of the two-degree-of-freedom oscillating cylinder at low mass ratios, less than $m^* = 6$ (Khalak and Williamson, 1996; Jauvtis and Williamson, 2003; Williamson and Govardhan, 2004). Jauvtis and Williamson (2004) found that for low damping and low mass ratio, the response of a circular cylinder free to vibrate in two directions can be very large, on the order of $A_y/D \approx 1.5$, forming a '2T' wake vortex structure, i.e. two triplets of vortices formed per cycle. The third vortex of the triplet, is a strong vortex, and the very large amplitude motions are attributed to the force contribution of this third vortex.

The purpose of the present experiments was to systematically explore the effects of low mass ratio and damping on a two-degree-of-freedom oscillating cylinder with varying in-line to transverse frequency ratio. Altering the natural frequency of the cylinder in the in-line direction significantly affects the cylinder response as shown by Sarpkaya (1995). Intermediate frequency ratios show a clear transition in the wake from the 1:1 frequency ratio case to the 2:1 frequency ratio case, while a low mass ratio shows an expanded response region in the nominal reduced velocity.

2. Experimental procedure

2.1. Experimental apparatus

A new apparatus was constructed to perform these tests at the MIT Towing Tank test facility. The testing tank is 2.4 m wide, 1.2 m deep, and has a useful test length of 22.5 m. A small carriage, riding on two steel rails, provides the mounting point for the test apparatus. A servo motor drives the carriage along the length of the tank at constant velocity.

The experimental apparatus connects to the carriage with a long, aluminum framework. The aluminum frame is positioned along the width of the tank, providing stability to the apparatus along the entire tank width. This framework

maximizes the span of the test cylinder. The moving portions of the test apparatus consist of four parts: guide bearing assembly, test cylinder assembly, spring bank, and linear motors. Fig. 1 shows the experimental apparatus connected to the towing carriage.

2.1.1. Guide bearing assembly

The guide bearing assembly is a set of roller bearings, mounted to a framework that allows motion in the vertical (transverse) and horizontal (in-line) directions. The horizontal assembly consists of four bearings mounted on two steel

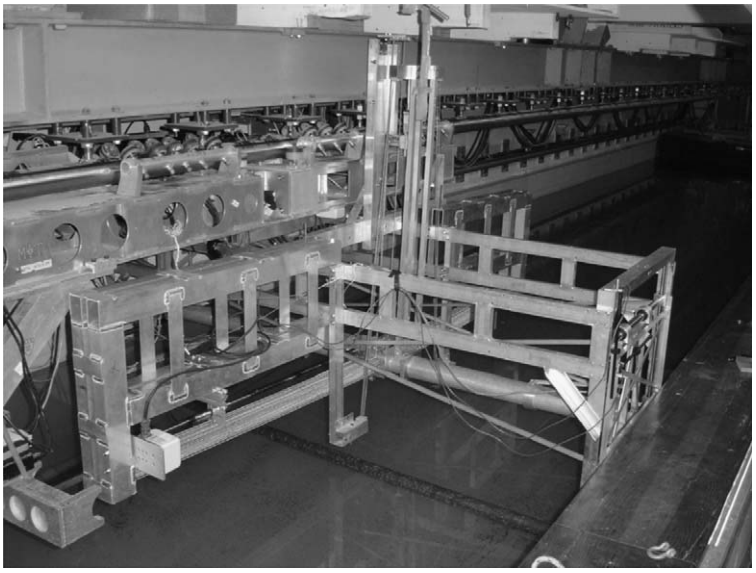

Fig. 1. Front view of the experimental apparatus.

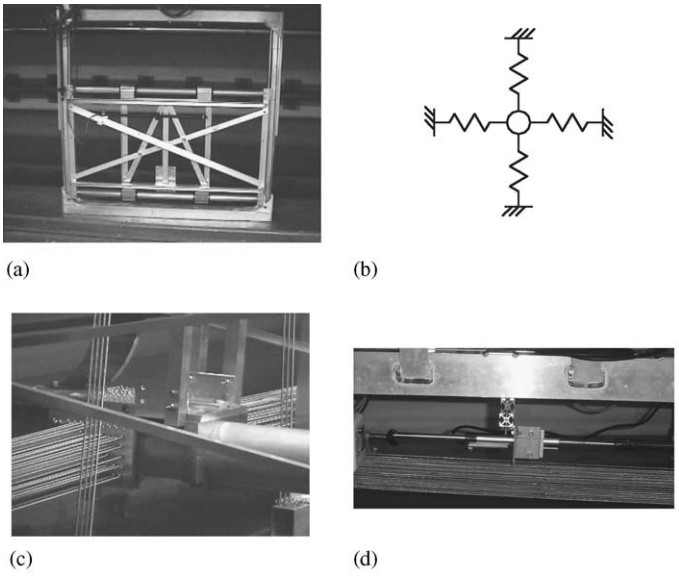

Fig. 2. Key components of the experimental apparatus: (a) Guide bearings; (b) spring bank schematic; (c) close-up of spring bank; (d) in-line linear motor.

shafts. The bearings are connected with thin, aluminum beams to maintain the relative distance between bearings. The horizontal framework is connected to four roller bearings, mounted vertically on two steel shafts. An outer framing stabilizes the vertical linear bearings. There is one guide bearing assembly on each side of the tank, connecting to the aluminum frame. The two guide bearing assemblies are tied together with aluminum angles, forming a box that moves as one piece. Fig. 2(a) shows the guide bearing assembly disconnected from the testing apparatus.

The guide bearing assemblies were constructed with lightweight parts in order to minimize the mass ratio in the experiment. Since the in-line bearing assembly is mounted to the transverse bearing assembly, the entire in-line assembly must move when there is motion in the transverse direction. This means that the mass ratio in the transverse direction will always be slightly higher than the mass ratio in the in-line direction. The two mass ratios have been kept as close as possible, since a cylinder in the field would typically have the same mass properties in both directions.

The roller bearings introduce friction in the system, making the structural damping of the experiment higher than desired. This friction is due to slight but unavoidable misalignments of the roller bearings over the large span of the test cylinder. Linear motors are used to offset this structural damping.

2.1.2. Test cylinder assembly

The test cylinder used in these experiments was a smooth, hollow, aluminum cylinder with a diameter of 7.62 cm and a span of 200 cm, giving an aspect ratio of 26. The test cylinder had piezoelectric force sensors mounted on each end of the cylinder. The force sensors were capable of measuring lift and drag forces.

The test cylinder was connected to two foil-shaped spars that extended through the free surface of the water and connected to the guide bearing assembly. A support cylinder connected the spars together at the guide bearing connection. The support cylinder also provided the connecting point for the spring bank and linear motors. All spring and motor forces were applied at the same point on the support cylinder.

End-plates were used on each end of the test cylinder. The end-plates were 45 cm in diameter and were centered along the centerline of the test cylinder. For frequency ratios greater than 1.6, the springs in the vertical direction were not strong enough to support the weight of the moving test apparatus. Therefore, it was necessary to install buoyancy plates for the frequency ratios of 1.67 and 1.9. The buoyancy plates, made of urethane foam, were connected to the outside of the end-plates, and were shaped like a bowl in order to minimize drag while maximizing buoyancy.

2.1.3. Spring bank

The spring bank allows fine tuning of the system natural frequency in both the in-line and transverse direction. The spring bank consists of four sets of extension springs that connect to the aluminum framework and the test cylinder assembly. The four sets of springs pull the cylinder forward, backward, upward, and downward. A schematic of the springs mounting to the test cylinder is shown in Fig. 2(b) and the actual spring connection to the cylinder is shown in Fig. 2(c). The four directions are necessary to center the test cylinder on the guide bearing rails. By connecting to the stationary framework and the moving test cylinder, the spring bank assembly provides a nonlinear spring constant in the transverse and in-line directions. Movement in the transverse direction will cause a spring deflection in the in-line direction and vice versa. This nonlinearity is minimized by using very long extension springs. The long extension springs allow a maximum spring deflection angle of 5°, which results in a maximum change in spring constant of less than 1% of the linear spring constant.

2.1.4. Linear motors

The presence of structural damping in the guide bearing assembly necessitated the use of linear motors to counter the damping force. Linear motors were connected in both the in-line and transverse directions. The motors were mounted on swivel hinges, allowing them to rotate with the motion of the cylinder. Carbon fiber tubing connected the linear motor shaft to the test cylinder assembly. The swiveling connection of the linear motors to the test cylinder causes a coupling between transverse motor forcing and in-line motor forcing. In order to minimize the effects of this coupling, the motors were placed as far from the cylinder as possible. The swivel hinge and in-line motor can be seen in Fig. 2(d).

The actual damping force in the bearings is difficult to measure because it changes with time, system use, and system setup. The bearings cause a stiction force, making the damping force difficult to quantify. A simplified predictive damping force model was used for the motor force output. The damping force models for the transverse (y-direction) and in-line (x-direction) motions were as follows, where $F_{y\,\mathrm{motor}}$ is the transverse motor force, and $F_{x\,\mathrm{motor}}$ is the in-line motor force:

$$F_{y\,\mathrm{motor}} = C_1\dot{y} + C_2\,\mathrm{sgn}(\dot{y})|\dot{y}|^p, \tag{1}$$

$$F_{x\,\mathrm{motor}} = C_3\dot{x} + C_4\,\mathrm{sgn}(\dot{x})|\dot{x}|^p; \tag{2}$$

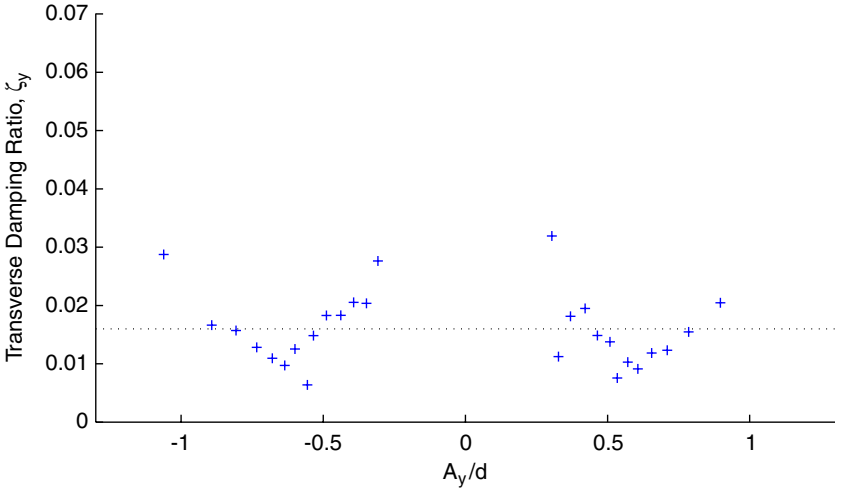

Fig. 3. Transverse damping as a function of A_y/D for a frequency ratio of 1.52. Dotted line indicates the mean value of damping.

C_1 and C_3 are gains for countering the linear damping in the system, which is primarily due to flexing structural components in the bearings. C_2 and C_4 are gains for countering the nonlinear damping in the system. This portion of the motor force is modeled as Coulomb damping, where there is a constant force opposing the direction of motion. This friction is apparent in the bearings where there is surface contact between the bearing rollers and the rails. The constant p is a number less than 0.5, which determines the smoothness of the function's transition through zero velocity. The velocity of the cylinder was measured in the transverse and in-line directions using linear velocity transducers. All natural frequency measurements were done in water. Conservative values for motor gains were chosen to avoid putting net energy into the system.

Fig. 3 shows the calculated transverse damping as a function of A_y/D for frequency ratio 1.52. With this apparatus, damping is a function of both time and amplitude. Due to quick amplitude decay, damping in theses tests can only be calculated per cycle for nondimensional amplitudes less than one. For this reason, damping is reported as the mean value of damping per cycle.

2.2. Test matrix

The system was tuned to six different frequency ratios and towed at nominal reduced velocities between 3 and 12. The frequency ratio is defined as the ratio between the in-line natural frequency and the transverse natural frequency. For each frequency ratio, a stiffness test was performed to determine the spring constant in each direction. The moving mass in each direction was calculated from the stiffness and frequency in each direction. Damping in still water was also determined from pluck tests. The structural characteristics for each frequency ratio are shown in Table 1, where f_{ny} is the transverse natural frequency, ζ_y is the mean transverse damping, ζ_x is the mean in-line damping, m_y^* is the transverse mass ratio, m_x^* is the in-line mass ratio, and $m_y^*\zeta_y$ is the mass-damping parameter.

3. Results

3.1. Cylinder orbits

Fig. 4 shows the orbital plot (in-line versus transverse motion) for each experiment. The horizontal axis shows the nominal reduced velocity, while the vertical axis shows the frequency ratio. The plotted orbital sequences include the time trace of the entire run along the length of the tank, excluding acceleration and deceleration times. For certain cases the cylinder did not repeat the same path from cycle to cycle and even drifted from one mode to another; hence certain plots appear more confused than other, purely periodic ones. The maximum attainable A_y/D with this apparatus was 1.35. In some cases, the cylinder occasionally reached the end of the guide bearing railing. These cases have been noted with an asterisk ($*$) in Fig. 4.

Table 1
Tuned frequency ratios

Ratio	f_{ny} (Hz)	ζ_y (%)	ζ_x (%)	m_y^*	m_x^*	$m_y^*\zeta_y$
1.00	0.715	2.2	2.2	3.8	3.3	0.084
1.22	0.799	1.3	1.7	3.9	3.8	0.051
1.37	0.894	1.1	2.5	3.9	3.7	0.043
1.52	0.977	1.6	3.2	4.0	3.6	0.064
1.67	0.698	2.6	2.9	5.5	5.3	0.14
1.90	0.704	6.2	2.5	5.7	5.0	0.35

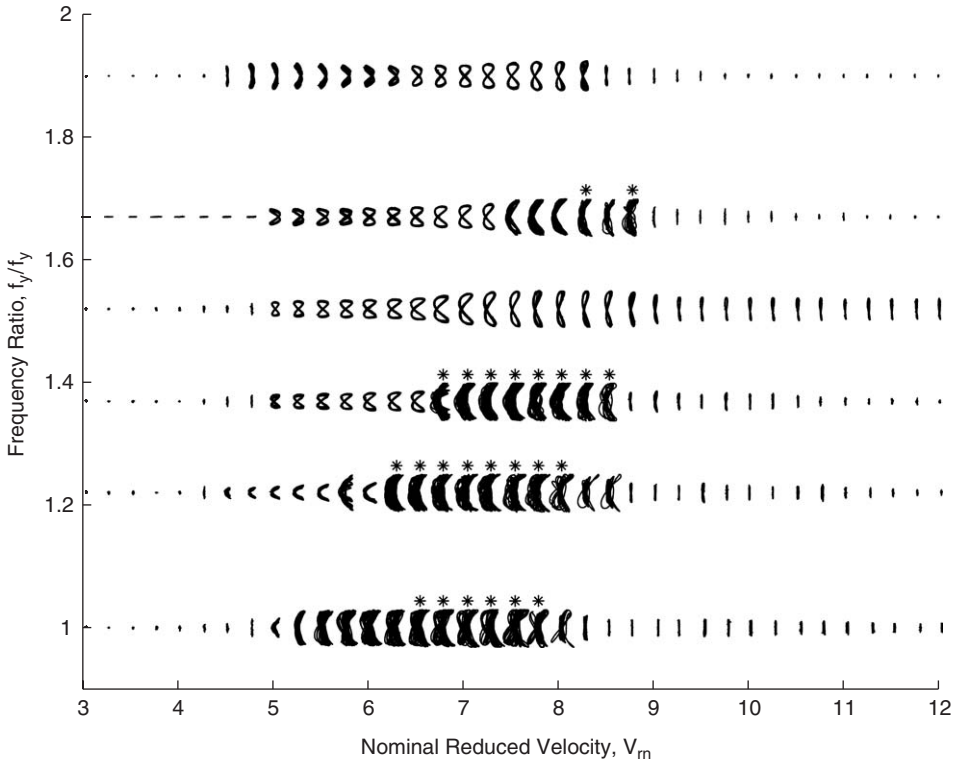

Fig. 4. Cylinder orbitals at varying frequency ratios: $*$ indicates cylinder motions were larger than $A_y/D = 1.35$.

3.2. Cylinder amplitude and frequency

Fig. 5 shows the transverse and in-line amplitudes of motion as well as the dominant oscillation frequency in the transverse and in-line directions. All motion amplitudes are reported as the mean of the top 10% of amplitudes over a given run. A dotted line has been drawn on Fig. 5 to signify runs where the apparatus reached the end of the guide railing and amplitudes are greater than $A_y/D = 1.35$. It is important to note in Fig. 5, that for each set of experiments, the damping ratio and mass ratio were slightly different, as given by Table 1. Response curves with higher mass and damping tend to be pinched-in, with lower response amplitudes at reduced velocities further away from the structural natural frequency. Hence, it is difficult to directly compare specific amplitudes in Fig. 5 for differing frequency ratio; however, the location of response peaks can be compared directly.

The frequencies reported in Fig. 5 refer to the dominant frequency of motion. In some cases, particularly for a frequency ratio of 1.0, there were multiple dominant frequencies in the in-line direction. Fig. 5 only shows the largest

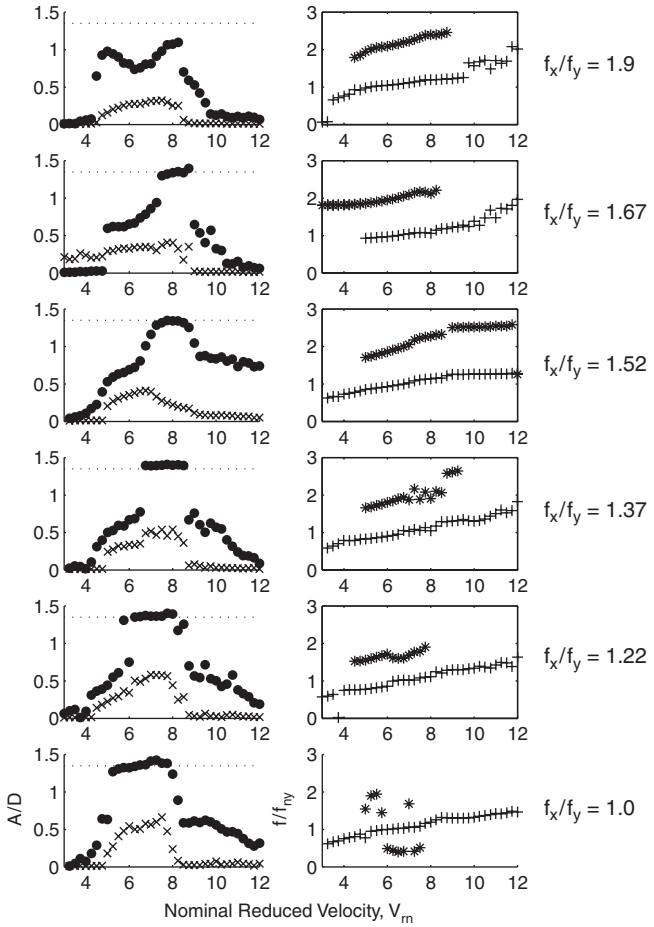

Fig. 5. Amplitude of cylinder motions and oscillation frequencies for different frequency ratios: •, transverse motion amplitude; ×, in-line motion amplitude; +, transverse motion frequency; ∗, in-line motion frequency.

magnitude frequency component in this case. Hence, there is a jump in in-line frequency for a frequency ratio of 1.0, where the nondimensional frequency jumps between 0.5,1.5, and 2. In reality, there are three frequency components apparent over the range of motions, but only the largest in magnitude is reported.

3.3. Comparison with other studies

We compare our results with the studies of Sarpkaya (1995) and Jauvtis and Williamson (2004). Fig. 6(a) shows the present results for a frequency ratio of 1.0, compared with similar tests performed by Sarpkaya (1995) and Jauvtis and Williamson (2004). The transverse motion amplitude is plotted on the vertical axis, while the parameter V_rSt is plotted on the horizontal axis. V_r is the true reduced velocity and St is the Strouhal number for the stationary cylinder in a uniform flow. For both the present study and Sarpkaya's (1995), the mass ratios were slightly different in each direction, while for Jauvtis and Williamson (2004) the mass ratio was the same in each direction. For the present study, the Reynolds number ranged from 16 000 to 60 000, while Sarpkaya (1995) cites a Reynolds number of 35 000 and Jauvtis and Williamson (2004) had a Reynolds number ranging from 7 200 to 15 400. The mass-damping parameter for the present study was 0.084 in this case. Mass-damping was not reported in Sarpkaya (1995), while the mass-damping for Jauvtis and Williamson (2004) was significantly lower than the present study, with a reported value of 0.0064.

Fig. 6(b) shows the present results, for frequency ratio 1.9, compared with the results of Sarpkaya (1995), for frequency ratio 2.0. Again, the mass ratios were slightly different in each direction for both sets of experiments.

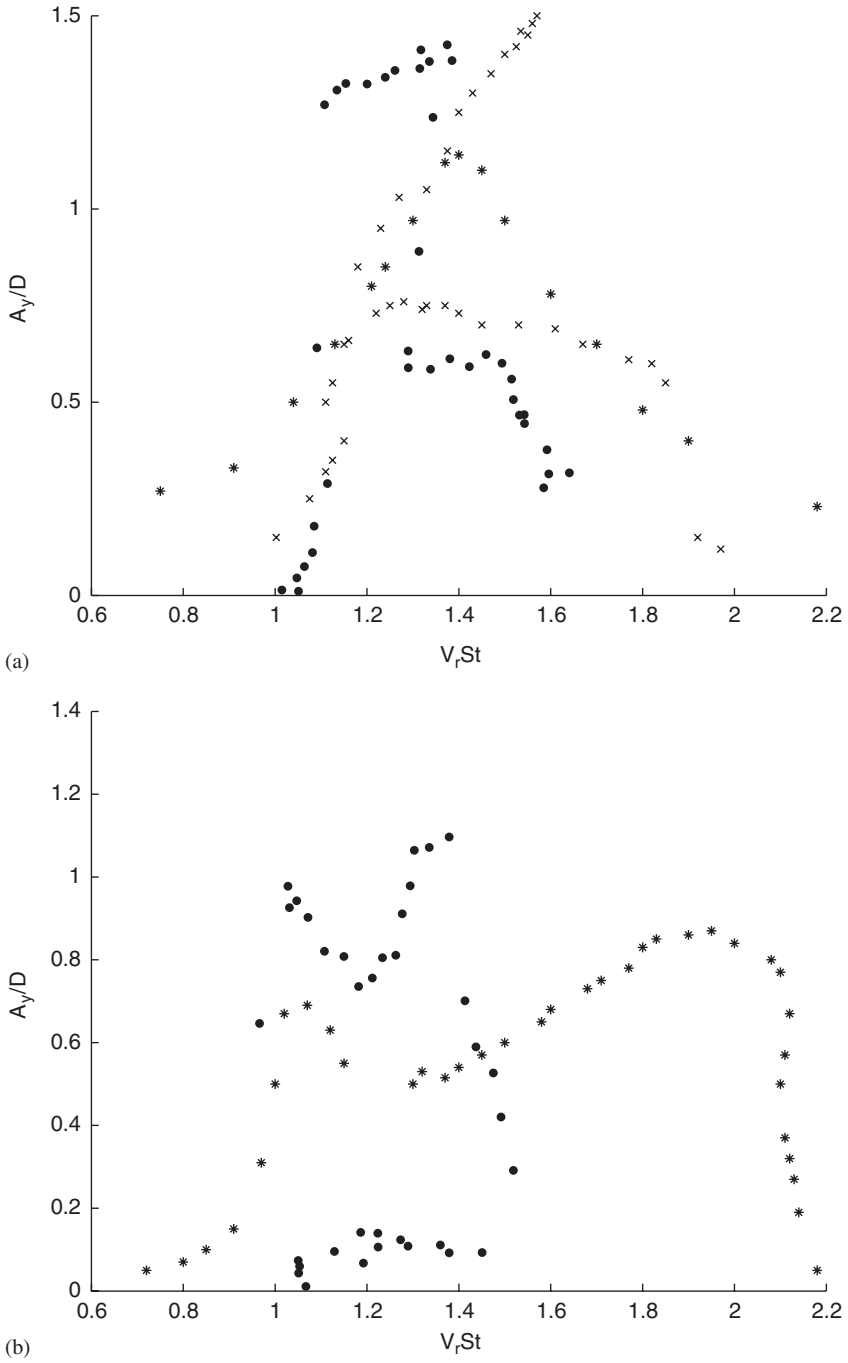

Fig. 6. Comparison of present study results with Sarpkaya (1995) and Jauvtis and Williamson (2004): •, present study; ∗, Sarpkaya (1995); ×, Jauvtis and Williamson (2004). (a) Frequency ratio = 1.0; (b) frequency ratio = 1.9 (2.0).

The Reynolds number in the present study ranged from 11 000 to 44 000, while the Reynolds number in Sarpkaya (1995) was 35 000. The mass-damping for the present study was fairly high, with a value of 0.35, while Sarpkaya (1995) did not report the mass-damping.

3.4. Average power balance

The flow of power in this experiment manifests itself in three forms: power from the fluid, power lost to linear and nonlinear damping, and power input from the linear motors. It is desirable that the power lost to structural damping equals the power input from the motor so that the average fluid power is zero. The fluid can act either as a source or a sink, removing power from the system or providing power to move the cylinder. Average fluid power is calculated as in Eq. (3), where T is the length of a test run, L is lift force, D is drag force fluctuation, $\dot{y}$ is transverse velocity, and $\dot{x}$ is in-line velocity fluctuation:

$$P_{\text{fluid}} = \frac{1}{T}\int_0^T (L\dot{y} + D\dot{x})\,\mathrm{d}t. \tag{3}$$

The total average power over one run must equal to zero:

$$0 = P_{\text{fluid}} + P_{\text{damping}} + P_{\text{motors}}. \tag{4}$$

If we assume a system with no damping, i.e. the linear motors have negated the damping in the system, then P_{fluid} must be equal to zero. P_{fluid} is known to be nonzero from the calculation in Eq. (3), hence damping cancelation is not exact. To quantify the error, we must first calculate the total power available in the system, P_{total}, estimated from the kinetic energy:

$$P_{\text{total}} = \max\left(\frac{\mathrm{d}}{\mathrm{d}t}\left(\frac{1}{2}m_y\dot{y}^2 + \frac{1}{2}m_x\dot{x}^2\right)\right). \tag{5}$$

We divide the error in power by the total power to generate a percent error, $\varepsilon_{\text{error}}$:

$$\varepsilon_{\text{error}} = \frac{P_{\text{fluid}}}{P_{\text{total}}}. \tag{6}$$

It is possible for $\varepsilon_{\text{error}}$ to be negative, referring to a system with negative damping. Zero $\varepsilon_{\text{error}}$ is indicative of a good test run. Positive $\varepsilon_{\text{error}}$ means that damping is positive. Large shown values of $\varepsilon_{\text{error}}$ correspond to small motions, which are overcome by the damping force. Since we cannot control the damping in the system perfectly and the pluck tests do not provide an accurate description of oscillatory damping, $\varepsilon_{\text{error}}$ was not always zero.

Fig. 7 shows the value of $\varepsilon_{\text{error}}$ for each frequency ratio. The error is less than 3% in most cases and has only been calculated for nondimensional amplitudes greater than 0.1.

4. Discussion

Changing the natural frequency in the in-line direction has a direct impact on the phase between the transverse response and the in-line response. If the transverse motion is equal to an amplitude times $\sin(\omega t)$, then the corresponding in-line motion is equal to an in-line amplitude times $\sin(2\omega t + \phi)$; ω is the frequency of motion, while ϕ is the phase between transverse and in-line motions. Fig. 4 shows that for a given nominal reduced velocity, the phase between transverse and in-line motions decreases as the frequency ratio increases.

Jeon and Gharib (2001) state that the cylinder motions have a higher power input with a phase angle of -45°, corresponding to a crescent-shaped figure eight with lobes facing downstream. This mode shape of the cylinder orbital pattern corresponds directly with the peak response of the cylinder for all frequency ratios. As frequency ratio increases, this peak response shifts to higher reduced velocity, where the drag excitation frequency is closer to the in-line natural frequency. The shift of the peak response is most clearly seen in Fig. 5. The peak response begins at a nominal reduced velocity of 5 for frequency ratio of 1.0. At frequency ratio of 1.67, the peak response begins at a nominal reduced velocity of 7.25. Jeon and Gharib (2001) found that the in-line motions of the cylinder can have a drastic effect on vortex shedding in the wake. They noted a disappearance of the '2P' shedding mode (four vortices per cycle) when the in-line motions were added to an equivalent transverse-only vibration which provided '2P' shedding. In-line cylinder motions actually delay the onset of the '2P' shedding mode due to the added accelerations of the cylinder in the in-line direction. By altering the frequency in the in-line direction, the cylinder accelerations are further modified, and the '2P' vortex mode is further delayed.

For a frequency ratio of 1.9, the transverse motion response shows two peaks in the response, as opposed to one peak seen in the other cases. In Fig. 4, one can see that at the first response peak, the cylinder is moving in an orbital shape with lobes facing upstream. This indicates that the phase between transverse and in-line motions has shifted to almost $+45^\circ$. This mode shape has similar accelerations to the -45° mode shape; hence, there is a peak in the response curve.

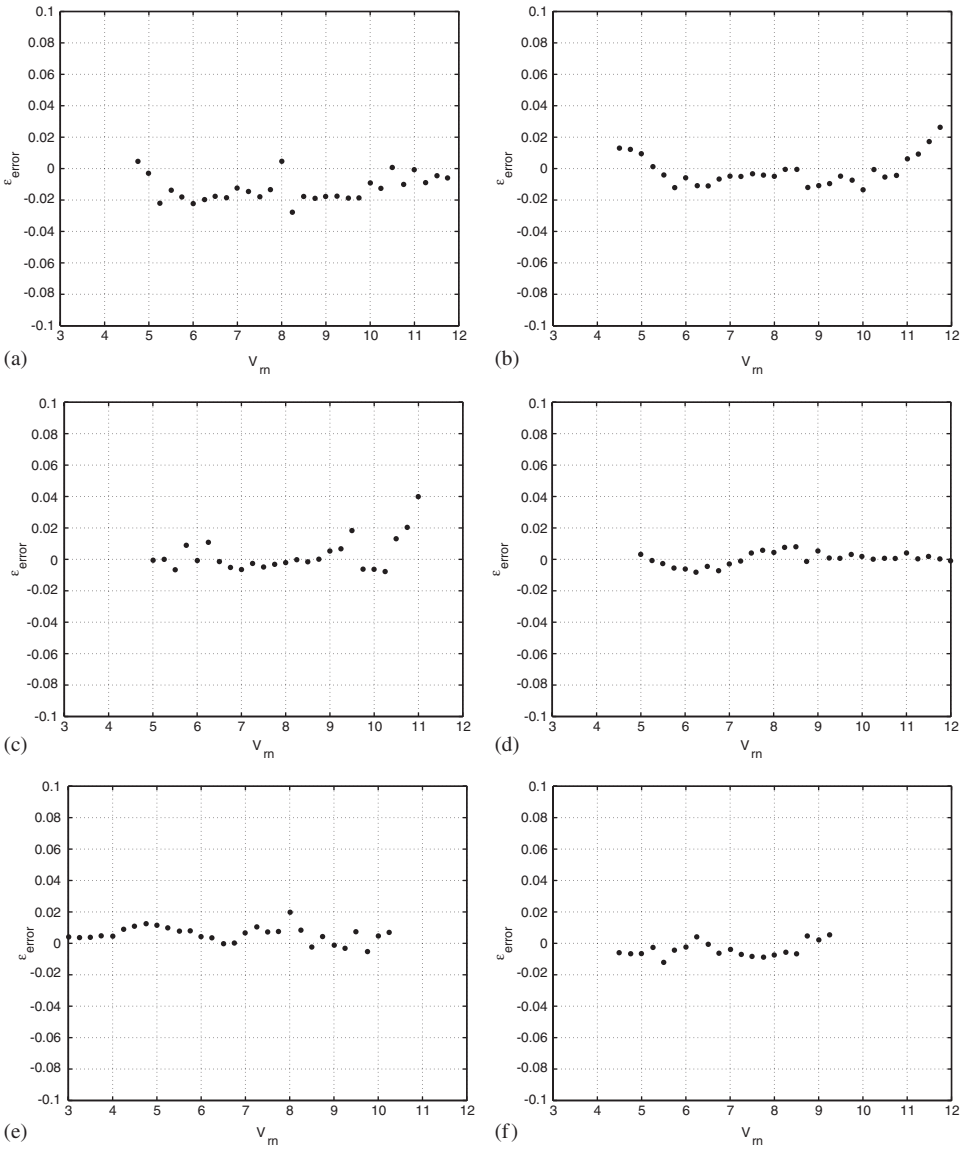

Fig. 7. Error in power balance for different frequency ratios: (a) frequency ratio = 1.0; (b) frequency ratio = 1.22; (c) frequency ratio = 1.37; (d) frequency ratio = 1.52; (e) frequency ratio = 1.67; (f) frequency ratio = 1.9.

A second peak occurs where the phase is -45°. This initial peak compares well with the response seen by Sarpkaya (1995), as shown in Fig. 6(b). The amplitudes are larger in the present study due to the smaller mass ratios, however Sarpkaya (1995) shows a much broader range of motion in the second response peak. Fig. 6(b) also shows a low amplitude overlap for the present study for V_rSt between 1.0 and 1.4. This overlapping region is a result of showing the amplitudes as a function of true reduced velocity. In Fig. 5, amplitude is shown as a function of nominal reduced velocity and there is no overlapping region. The low amplitude branch consists of points at high nominal reduced velocity, where the excitation frequency was far from the system natural frequency, thus amplitudes were small and damping forces were large in comparison to excitation forces.

Although the linear motors do reduce damping in this experiment, the damping force is nonlinear and is difficult to cancel exactly. The various tests presented were performed with different natural frequencies, therefore the speed range for each test was different in order to make appropriate nondimensional comparisons. Better results are obtained when the natural frequency of the system is higher, because the speed is also higher, resulting in larger lift forces. Since the damping force had generally the same magnitude for each run, larger lift forces overcome the structural damping more

easily. Table 1 shows the natural frequencies used in this experiment. The best results were obtained for a frequency ratio of 1.52, which incidentally corresponds to the highest tuned natural frequency. Frequencies are different for each run due to the coupling between in-line and transverse frequency from the spring bank.

The power error estimates shown in Fig. 7 help indicate which test runs are best. Overall, the error is very small compared to the power available to the system; however, the linear motors are not perfectly tuned to the damping characteristics and an error is still evident. The cylinder hit the end rails in some cases where the power error was very close to zero or slightly negative; while, in other cases, cylinder motions were almost nonexistent for large, positive power error. A negative power error does not indicate an unstable system, where the system would continually hit the ends of the guide rails. Instead, a negative power error indicates a slight surplus of power on average over the entire run. Thus, the guide rails were hit in some instances, but not continually over the entire test run. In the cases where power error was negative, the error was very small, less than 2% of the available power, so the results are still acceptable.

The maximum amplitudes compare well with the amplitudes observed by Jauvtis and Williamson (2004) in Fig. 6(a). Having a low mass ratio in two-degree-of-freedom oscillations can result in very large amplitude motions in excess of $A_y/D = 1.35$. It is important to note that the two sets of experiments were conducted at different Reynolds numbers, hence the Strouhal frequency is not the same. Also, the mass ratios in each direction were slightly different in the present study, whereas Jauvtis and Williamson (2004) used a system with equal mass ratio in each direction. This explains the slight location difference between the peak responses. The lower mass-damping in Jauvtis and Williamson (2004) also explains the broader region of reduced velocity in which large motions were observed, when compared with the observed region of motion in the present study. The lower branch of Jauvtis and Williamson (2004) matches well with a portion of the lower branch from the present study.

5. Conclusions

Systematic experiments were conducted on a flexibly mounted, towed, rigid cylinder, capable of oscillating in the in-line and transverse directions. The experiments were performed in order to study the cylinder response due to variation of in-line versus transverse frequency ratio. The cylinder aspect ratio was 26 and the Reynolds number ranged from 11 000 to 60 000.

The maximum overall transverse response exceeds $A_y/D = 1.35$, while the in-line response reaches up to $A_x/D = 0.6$. The response may consist of a single-pattern or multiple patterns, when switching between patterns is observed. The phase between transverse and in-line motions shifts and alters the cylinder orbit, causing this mode switching. Hence, the in-line response is found to govern the phase between the transverse and in-line motions, affecting the shape of the cylinder orbital pattern. For a frequency ratio of 1.0, the phase between transverse and in-line motions was seen to undergo a smooth transition from 0 degrees to -45° (figure-eight changing to crescent-shaped figure-eight facing downstream). The crescent-shaped mode results in the largest amplitude response, where power transfer between motions is at a maximum. At higher frequency ratios, the phase is shifted to more positive values. At a frequency ratio of 1.9 we observe an upstream crescent shape, corresponding to a distinct second response peak versus the nominal reduced velocity.

Linear motors are used to remove linear and nonlinear damping forces, so as to obtain a purely free vibration condition, i.e. with zero average fluid power input. Indeed, the measured power error was found to be small for most test runs.

References

Brika, D., Laneville, A., 1993. Vortex-induced vibrations of a long flexible circular cylinder. Journal of Fluid Mechanics 250, 481–508.

Govardhan, R., Williamson, C.H.K., 2000. Modes of vortex formation and frequency response of a freely vibrating cylinder. Journal of Fluid Mechanics 420, 85–130.

Jauvtis, N., Williamson, C.H.K., 2003. Vortex-induced vibration of a cylinder with two degrees of freedom. Journal of Fluids and Structures 17, 1035–1042.

Jauvtis, N., Williamson, C.H.K., 2004. The effect of two degrees of freedom on vortex-induced vibration at low mass and damping. Journal of Fluid Mechanics 509, 23–62.

Jeon, D., Gharib, M., 2001. On circular cylinders undergoing two-degree-of-freedom forced motions. Journal of Fluids and Structures 15, 533–541.

Khalak, A., Williamson, C.H.K., 1996. Dynamics of a hydroelastic cylinder with very low mass and damping. Journal of Fluids and Structures 10, 455–472.

Moe, G., Wu, Z.-J., 1990. The lift force on a cylinder vibrating in a current. Journal of Offshore Mechanics and Arctic Engineering 112, 297–303.

Sarpkaya, T., 1979. Vortex-induced oscillations. Journal of Applied Mechanics 46, 241–258.

Sarpkaya, T., 1995. Hydrodynamic damping, flow-induced oscillations, and biharmonic response. ASME Journal of Offshore Mechanics and Arctic Engineering 117, 232–238.

Sarpkaya, T., 2004. A critical review of the intrinsic nature of vortex-induced vibrations. Journal of Fluids and Structures 19, 389–447.

Williamson, C.H.K., Govardhan, R., 2004. Vortex-induced vibrations. Annual Review of Fluid Mechanics 36, 413–455.

Williamson, C.H.K., Roshko, A., 1988. Vortex formation in the wake of an oscillating cylinder. Journal of Fluids and Structures 2, 355–381.